890. Forecasting control of adjacent structures based on optimal grey model

L. H. Zou[1], K. Huang[2]
School of Civil Engineering, Fuzhou University, Fuzhou, 350108, China
E-mail: [1]*Zoulihua66@163.com*, [2]*huangkaie@qq.com*

(Received 30 June 2012; accepted 4 December 2012)

Abstract. The purpose of this paper is to investigate the forecasting control of adjacent buildings with optimal grey model (GM). Firstly, based on the linear quadratic regulator (LGR) control, a novel forecasting control scheme for adjacent buildings using optimal GM is proposed, the calculation model is established, and the motion and control equations are derived. Secondly, a numerical investigation of a complex system with two adjacent buildings is conducted, and the influence of time delay on control of adjacent buildings is analyzed. Finally, the effect of forecasting control on the time delay of adjacent buildings is studied. The numerical results indicate that the forecasting control method based on optimal GM is reliable and practical in vibration control of buildings, particularly in the case of adjacent buildings.

Keywords: forecasting control, optimal GM, time delay, adjacent buildings.

Introduction

Pounding problem of adjacent buildings occurs when the lateral space between the buildings is not to allow the buildings to vibrate freely. Due to the mass of buildings, the momentum of the vibrating structure is quite large and can result in significant local damage or even total collapse of the buildings during pounding. A survey [1] of 330 collapsed or severely damaged buildings during the 1985 Mexico earthquake has revealed that pounding was present in over 40 % of these buildings and in 15 % of all cases it led to collapse. Kasai and Maison [2] have surveyed the damage from pounding in the San Francisco Bay area during the 1989 Loma Prieta earthquake. Pounding was wide-spread in the Bay area, and significant pounding was observed in the area of 90 km from the epicenter. Similar scenario of pounding has also been reported during 1994 Northridge earthquake [3].

To prevent mutual pounding between adjacent buildings during an earthquake, Westermo [4] analyzed the seismic behavior of adjacent buildings connected by hinged rigid links. Kobori [5] et al developed bell-shaped hollow connectors to link adjacent buildings. The bell-shaped hollow connector is made of steel with stabilized hysteretic characteristic, which can absorb vibration energy of the buildings during strong earthquakes. Basili and Angelis [6] studied the optimal passive control of adjacent structures interconnected with nonlinear hysteretic devices. Although all these methods can reduce the response of system and the chance of pounding, the effect of these methods depends on the dynamic characteristics of system excessively.

Some scholars [7-9] proposed to link the adjacent structures with control devices and apply active or semi-active control to them. The linear quadratic control method was employed in most of these studies. But when developing large-scale practical applications, a number of problems rose due to the consequences of time-delay within the control of adjacent buildings system. The control precision of linear quadratic control method relies on an accurate structural model. It is more difficult to construct an accurate model of adjacent buildings than in the case of a single building. As a result, it will produce a larger time-delay when the adjacent building is controlled. A small time-delay may only reduce the potential benefits of the control process, whereas a large time-delay may cause failure of the control process, or even lead to possible magnification of the structural response and collapse of the host structure.

Two common methods for solving the time-delay problem are the time-delay compensation method and the forecasting control method [10]. A number of time-delay compensation

methods [10] have been studied numerically and experimentally, but its limitations can not be overcome. For example, the controller is often derived on the basis of modified state feedback without simultaneous consideration of the time-delay effect. Therefore, the result is that system stability cannot be guaranteed, especially when the time-delay becomes large.

The forecasting control method is one of the more effective methods for mitigating the effects of time-delay. Grey forecasting is one of the forecasting theories that has been successfully applied to a variety of problems [10-15]. It is independent of accurate structural models and need only a few samples. This is quite suitable to be used as a structural model predictor and controller, particularly in the situation when the actual system is complex and large.

The purpose of this paper is to investigate the control of adjacent buildings employing grey forecasting model. Based on the linear quadratic regulator control, an novel forecasting control scheme of adjacent buildings using optimal grey model is proposed, the calculation model is established, and the motion and control equations are derived. By numerical study conducted on a complex system of two adjacent buildings, the influence of time delay on control of adjacent buildings are analyzed, and the effect of forecasting control on the time delay of adjacent buildings is studied.

1. Equation of motion for adjacent buildings

The building model of a complex and the respective analytical model are shown in Fig. 1 and 2. Structure A is an n_1-storey fixed-base building, and structure B is an n_2-storey isolation building. They are linked by some control devices. The equations of structure A and B are given by:

$$\mathbf{M}_1\ddot{\mathbf{x}}_1 + \mathbf{C}_1\dot{\mathbf{x}}_1 + \mathbf{K}_1\mathbf{x}_1 = -\mathbf{M}_1\mathbf{I}_1\ddot{x}_g + \mathbf{H}_1\mathbf{u} \tag{1}$$

$$\mathbf{M}_2\ddot{\mathbf{x}}_2 + \mathbf{C}_2\dot{\mathbf{x}}_1 + \mathbf{K}_2\mathbf{x}_2 = -\mathbf{M}_2\mathbf{I}_2\ddot{x}_g - \mathbf{H}_2\mathbf{u} \tag{2}$$

where, $\mathbf{M}_1$, $\mathbf{C}_1$ and $\mathbf{K}_1$ are mass, damping and stiffness matrices of structure A, respectively; $\ddot{\mathbf{x}}_1$, $\dot{\mathbf{x}}_1$ and $\mathbf{x}_1$ are acceleration, velocity and displacement vectors of structure A, respectively; $\mathbf{M}_2$, $\mathbf{C}_2$ and $\mathbf{K}_2$ are mass, damping and stiffness matrices of structure B, respectively; $\ddot{\mathbf{x}}_2$, $\dot{\mathbf{x}}_2$ and $\mathbf{x}_2$ are acceleration, velocity and displacement vectors of structure B, respectively; $\mathbf{I}_1$ and $\mathbf{I}_2$ are n_1 and (n_2+1) - dimensional identity vectors; $\mathbf{H}_1$ and $\mathbf{H}_2$ are the location matrices of control force; $\ddot{x}_g$ is the acceleration of ground. Eq. (1) and (2) can be rewritten as:

$$\mathbf{M}\ddot{\mathbf{x}} + \mathbf{C}\dot{\mathbf{x}} + \mathbf{K}\mathbf{x} = -\mathbf{M}\mathbf{I}\ddot{x}_g + \mathbf{H}\mathbf{u} \tag{3}$$

where:

$$\mathbf{M} = \begin{bmatrix} \mathbf{M}_1 & \\ & \mathbf{M}_2 \end{bmatrix};\ \mathbf{K} = \begin{bmatrix} \mathbf{K}_1 & \\ & \mathbf{K}_2 \end{bmatrix};\ \mathbf{C} = \begin{bmatrix} \mathbf{C}_1 & \\ & \mathbf{C}_2 \end{bmatrix};$$

$\ddot{\mathbf{x}}$, $\dot{\mathbf{x}}$ and $\mathbf{x}$ are the equivalent acceleration, velocity and displacement vectors of the system; $\mathbf{H}$ is the equivalent location matrix of system, $\mathbf{u}$ is the vector of control force.

In state space, Eq. (3) becomes:

$$\dot{\mathbf{Z}} = \mathbf{A}\mathbf{Z} + \mathbf{B}\mathbf{u} + \mathbf{E} \tag{4}$$

where:

$$\mathbf{Z}=\begin{bmatrix}\mathbf{x}\\ \dot{\mathbf{x}}\end{bmatrix},\ \mathbf{A}=\begin{bmatrix}\mathbf{0} & \mathbf{0} & \mathbf{I} & \mathbf{0}\\ \mathbf{0} & \mathbf{0} & \mathbf{0} & \mathbf{I}\\ -\mathbf{M}_1^{-1}\mathbf{K}_1 & 0 & -\mathbf{M}_1^{-1}\mathbf{C}_1 & \mathbf{0}\\ \mathbf{0} & -\mathbf{M}_2^{-1}\mathbf{K}_2 & \mathbf{0} & -\mathbf{M}_2^{-1}\mathbf{C}_2\end{bmatrix},\ \mathbf{B}=\begin{bmatrix}\mathbf{0}\\ \mathbf{0}\\ \mathbf{M}_1^{-1}\mathbf{H}_1\\ -\mathbf{M}_2^{-1}\mathbf{H}_2\end{bmatrix},\ \mathbf{E}=\begin{bmatrix}\mathbf{0}\\ \mathbf{0}\\ -\mathbf{I}\ddot{\mathbf{x}}_g\\ -\mathbf{I}\ddot{\mathbf{x}}_g\end{bmatrix}$$

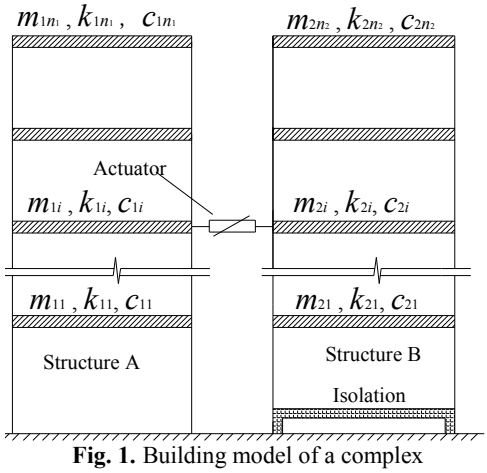

Fig. 1. Building model of a complex

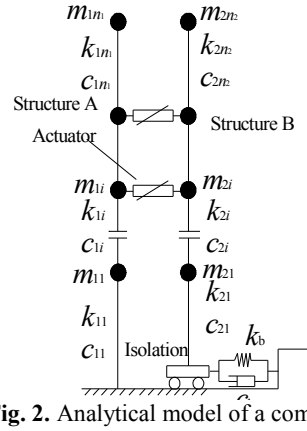

Fig. 2. Analytical model of a complex

2. Forecasting control based on optimal grey model

2. 1. Design of control scheme

As shown in Fig. 3, the working process of control in the case of earthquake excitation is as follows. In general, as seismic ground motion is initiated, the magnitude of the response is usually small, but sufficient to cause the sampling devices to start operating. A series of structural response data values (e.g. $\boldsymbol{Z}(t_k)$, where $\boldsymbol{Z}(t_k)$ can represent displacements, velocities accelerations or control forces) are measured and transmitted to the grey forecasting device for determining the forecast value $\boldsymbol{Z}(t_k + \Delta t)$ (Δt represents the time-delay of the system). $\boldsymbol{Z}(t_k + \Delta t)$ is transmitted to the comparator and compared with the target value. The control vector $\boldsymbol{U}$ is determined based on $\boldsymbol{Z}(t_k + \Delta t)$ and the target value and then output to the actuators. Based on $\boldsymbol{U}$, the actuators apply the control forces to the structure. The next state vectors $\boldsymbol{Z}(k + 1)$ for modeling will be generated, measured by the sampling device as new data and input into the next forecasting control cycle. The cycles continue until the ground excitation or response smaller than a predetermined value and the control process ends.

2. 2. Forecasting model

Principle of grey forecasting model. The working process of a grey forecasting control system is shown in Fig. 4. The output vector $\boldsymbol{Y}$ is measured continuously by a sampling device after the values of $\boldsymbol{Y}$ at the time of the k^{th} step are forecast. Then it fed back by the grey forecasting device and compared with target values in terms of system time-delay. After that the control signal (CS) is generated with the objective of making the future output $\boldsymbol{Y}$ close to target value $\boldsymbol{J}$. Finally, the actuator accepts the CS and applies the control force to the building. The

whole control system includes four subsystems: the sampling system, the forecasting system, the control system, and the mechanical force system.

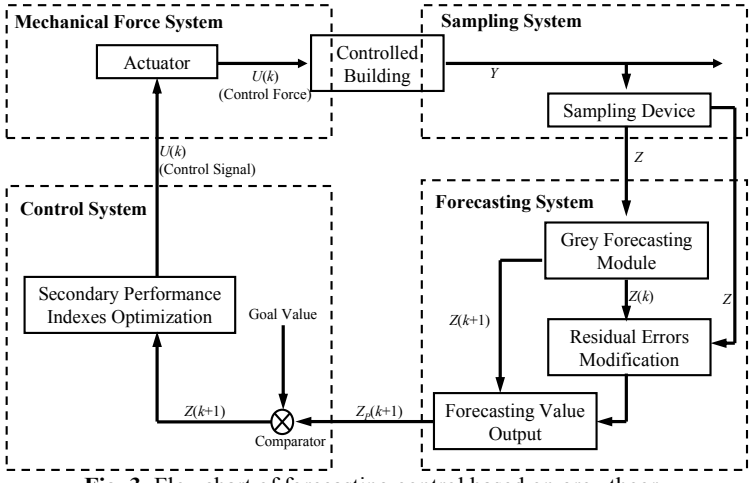

Fig. 3. Flowchart of forecasting control based on grey theory

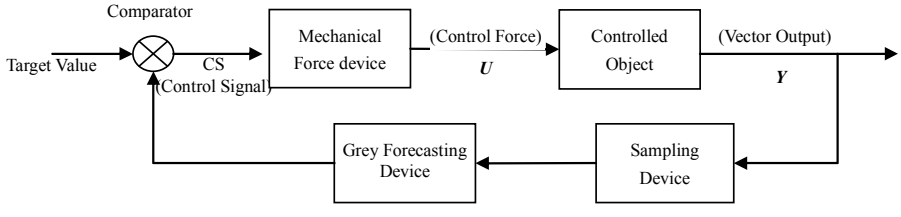

Fig. 4. Flowchart of grey forecasting control process

Grey theory forecasting model. When applying forecasting control, forecasting is obviously the key process within the control system. In this paper, optimal grey forecasting is presented by the flowchart presented in Fig. 5. The process starts with the collection of original data by the data collecting module. After required equal interval treatment and the pretreatment of the data series, the input data can satisfy demands of the GM(1,1) model and the forecast values of the next step can be generated from the forecast model.

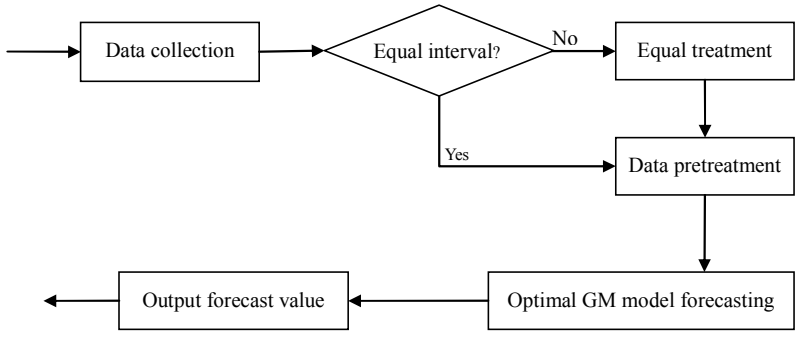

Fig. 5. Flowchart of grey forecasting model

Considering $\boldsymbol{Z}(t)$ as the state vector sample of the system at the present time, and $\boldsymbol{Z}(t-3)$, $\boldsymbol{Z}(t-2)$ and $\boldsymbol{Z}(t-1)$ as samples at earlier times, the raw series can be written as:

$$Z^{(0)}(k) = Z(t+k-4) \qquad (k = 1,2,3,4) \tag{5}$$

Abbreviating the Accumulating Generation Operation as AGO, which is denoted to generate a series through successively adding raw data in series, the AGO series of $\boldsymbol{Z}^{(1)}$ can be written as:

$$Z^{(1)}(k) = \mathrm{AGO} \cdot Z^{(0)} = \sum_{i=1}^{k} Z^{(0)}(i) \qquad (k = 1,2,3,4) \tag{6}$$

The neighboring mean value series $w^{(1)}$ is defined as:

$$w^{(1)}(k) = \frac{1}{2}\left[Z^{(1)}(k) + Z^{(1)}(k-1) \right] \qquad (k = 2,3,4) \tag{7}$$

From the generating series $\boldsymbol{Z}^{(1)}(k)$, a white differential equation may be obtained as:

$$\frac{dZ^{(1)}}{dt} + A_g Z^{(1)} = B_g \tag{8}$$

where A_g is the developing coefficient and B_g is the grey input.

The distinguishing parameter vectors $\hat{a} = [A_g, B_g]^T$ may be obtained by the least squares method:

$$\hat{a} = \begin{bmatrix} A_g \\ B_g \end{bmatrix} = (V^T V)^{-1} V^T Y_n \tag{9}$$

where V is a $6n \times 4n$ dimensional matrix and $\boldsymbol{Y}_n$ is a $6n$ dimensional vector. $\boldsymbol{V}_n$, $\boldsymbol{Y}_n$ can be assembled as:

$$V = \begin{bmatrix}
w^{(1)}(2,1) & 1 & & & & & & 0 \\
w^{(1)}(3,1) & 1 & & & & & & \\
w^{(1)}(4,1) & 1 & & & & & & \\
 & & w^{(1)}(2,2) & 1 & & & & \\
 & & w^{(1)}(3,2) & 1 & & & & \\
 & & w^{(1)}(4,2) & 1 & & & & \\
 & & & & \ddots & & & \\
 & & & \ddots & & & & \\
 & & & & & & & \\
 & & & & & w^{(1)}(2,n) & 1 & \\
 & & & & & w^{(1)}(3,n) & 1 & \\
0 & & & & & w^{(1)}(4,n) & 1 &
\end{bmatrix}, \quad Y_n = \begin{bmatrix}
Z^{(0)}(2,1) \\
Z^{(0)}(3,1) \\
Z^{(0)}(4,1) \\
Z^{(0)}(2,2) \\
Z^{(0)}(3,2) \\
Z^{(0)}(4,2) \\
\vdots \\
\vdots \\
 \\
Z^{(0)}(2,n) \\
Z^{(0)}(3,n) \\
Z^{(0)}(4,n)
\end{bmatrix}$$

The solution of the white differential equation can be expressed as:

$$\dot{Z}^{(1)}(k+1) = (Z^{(0)}(1) - B_g \cdot / A_g)e^{-A_g k} + B_g \cdot / A_g \tag{10}$$

Applying an inverse accumulating generation operation (IAGO) to $\dot{Z}^{(1)}(k)$, the forecast value of the next step can be obtained as:

$$\dot{Z}^{(0)}(k+1) = \text{IAGO} \cdot \dot{Z}^{(1)}(k+1) - \dot{Z}^{(1)}(k) \tag{11}$$

After the forecast data has been retrieved and modified to diminish residual error, the final forecast value is obtained as:

$$Z^{(0)}(k+1) = -A_g \cdot (Z^{(0)}(1) - B_g \cdot / A_g) \cdot e^{-A_g k} \pm A_\varepsilon \cdot (\varepsilon^{(0)}(k_0) - B_\varepsilon \cdot / A_\varepsilon) \cdot e^{-A_\varepsilon (k-k_0)} \tag{12}$$

where $\varepsilon^{(0)}(k) = Z^{(0)}(k) - \dot{Z}^{(0)}(k)$, the calculation methods for A_ε, B_ε are the same as for A_g, B_g, and k_0 is the number of raw data series.

The grey forecasting algorithm is based on the metabolizing model, where the input $Z^{(0)}$ is constantly updated by replacing old data with the newest data. Thus good adaptability of the model is ensured.

The background value is one of the key factors influencing the control process. Based on the exponential function form of the model, the background value may be determined by an integral formula, allowing the original background value to be optimized. Hence a modified grey forecasting model based on the optimal background value can improve the forecast precision and overcome the delay errors arising in the original gray forecasting model.

From Eq. (12), the simulation and prediction precision of the GM(1,1) model depend on parameters A_g, and B_g, which in turn rely on the raw data series and form of the background value $w^{(1)}(k)$. $w^{(1)}(k)$ is one of the key factors influencing the simulation error $[\varepsilon^{(0)}(k) = \hat{Z}^{(1)}(k) - Z^{(1)}(k)]$ and the applicability of the GM(1,1) model.

Thus Eq. (8) may be integrated from k to $k + 1$ (Fig. 6):

$$Z^{(1)}(k+1) - Z^{(1)}(k) + A_g \int_k^{k+1} Z^{(1)}(t)dt = B_g \qquad k = 1, 2, \cdots, n-1 \tag{13}$$

Assuming $w^{(1)}(k + 1)$ is the background value of $z^{(1)}(t)$ in the interval $[k, k + 1]$, it can be obtained as:

$$\int_k^{k+1} z^{(1)}(t)dt = \left[(k+1) - k\right] w^{(1)}(k+1) = w^{(1)}(k+1) \tag{14}$$

Eq. (14) shows that the background value is the definite integral of $z^{(1)}(t)$ in the interval $[k, k + 1]$.

Because the solution of Eq. (8) is in exponential form, $z^{(1)}(t)$ can be written as:

$$z^{(1)}(t) = ce^{bt} \tag{15}$$

with the curve passing through the points $z^{(1)}(k)$ and $z^{(1)}(k + 1)$, thus:

$$z^{(1)}(k) = ce^{bk} \tag{16}$$

$$z^{(1)}(k+1) = ce^{b(k+1)} = ce^{bk} \cdot e^{b} \tag{17}$$

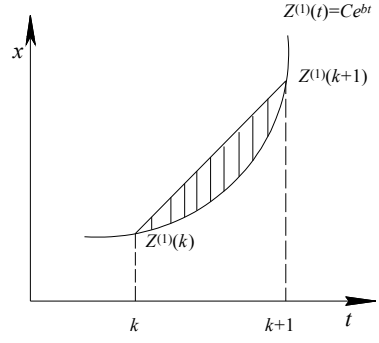

Fig. 6. A schematic diagram presenting reasons for error from original model GM(1,1)

From Eq. (16) and Eq. (17) we have:

$$b = \ln\left[\frac{z^{(1)}(k+1)}{z^{(1)}(k)}\right] = \ln z^{(1)}(k+1) - \ln z^{(1)}(k) \tag{18}$$

$$c = \frac{z^{(1)}(k)}{e^{bk}} = \frac{z^{(1)}(k)^{k+1}}{z^{(1)}(k+1)^{k}} \tag{19}$$

Thus optimal background value is:

$$w^{(1)}(k+1) = \int_{k}^{k+1} z^{(1)}(t)dt = \int_{k}^{k+1} ce^{bt}dt = \frac{c}{b}(e^{b(k+1)} - e^{bk}) = \frac{z^{(1)}(k+1) - z^{(1)}(k)}{\ln z^{(1)}(k+1) - \ln z^{(1)}(k)} \tag{20}$$

Let:

$$y_n = \left[z^{(0)}(2), z^{(0)}(3), z^{(0)}(4), \cdots, z^{(0)}(n)\right]^T \tag{21}$$

$$B = \begin{pmatrix} -w^{(1)}(2) & 1 \\ -w^{(1)}(3) & 1 \\ \cdots & \cdots \\ -w^{(1)}(n) & 1 \end{pmatrix} \tag{22}$$

The parameter vectors $\hat{a} = [A_g, B_g]^T$ can be obtained by the least squares method as:

$$\hat{a} = \left[B^T B\right]^{-1} B^T y_n \tag{23}$$

Substituting Eq. (23) into Eq. (8), and letting and $z^{(1)}(t)_{t=1} = z^{(0)}(1)_{t=1}$, it can be obtained:

$$\hat{Z}^{(1)}(t)=\left[Z^{(0)}(1)-\frac{B_g}{A_g}\right]e^{-A_g(t-1)}+\frac{B_g}{A_g} \tag{24}$$

For AGO series $X^{(1)}(k)$, we have:

$$\hat{Z}^{(1)}(k+1)=\left[Z^{(0)}(1)-\frac{B_g}{A_g}\right]e^{-A_g k}+\frac{B_g}{A_g} \tag{25}$$

In Eq. (25), $\hat{Z}^{(1)}(k)$ is determined by means of an Inverse Accumulated Generating Operation (IAGO). Therefore, the value of $Z^{(0)}(k)$ can be predicted as:

$$\begin{cases}\hat{Z}^{(0)}(1)=Z^{(0)}(1)\\ \hat{Z}^{(0)}(k+1)=\hat{Z}^{(1)}(k+1)-\hat{Z}^{(1)}(k)=(1-e^{A_g})\left[Z^{(0)}(1)-\dfrac{B_g}{A_g}\right]e^{-A_g k}\end{cases} \tag{26}$$

3. Control equation and solution

The classical LQR method is employed to design the controllers. The index of control performance can be expressed as:

$$J=\frac{1}{2}\{Z-\alpha\}^T S\{Z-\alpha\}+\frac{1}{2}\int_0^{t_f}\{Z-\beta\}^T Q\{Z-\beta\}+u^T dt \tag{27}$$

where S, Q are $2n \times 2n$ weighting matrices of response; R is $n \times n$ weighting matrix of control force; t_f is time of the control end; α is $n \times n$ expected steady response vector in t_f; β is $n \times 1$ expected instantaneous response vector in t_f. Assuming $t_f=\infty$, $\lim_{t_f\to 0} Z=0$, $\alpha=0$, $\beta=0$, Eq. (27) can be rewritten as:

$$J=\frac{1}{2}\int_0^{t_f} Z(t)^T QZ(t)+U^T RU(t)dt \tag{28}$$

Generally, the performance of an optimal closed-loop control system is determined by the ratio of Q and R. Increasing Q or reducing R will increase the control force, enhance the gain feedback of control system, thus decreasing the amplitude of dynamic responses. Therefore a reasonable determination of Q and R will be very important for the design of the control system. In this paper, Q and R are determined by:

$$Q=\alpha_1\begin{bmatrix}K & \\ & M\end{bmatrix},\ R=\beta_1 I \tag{29}$$

where α_1, and β_1 are the undetermined coefficients related to the constants of controller, which are used to adjust the values of Q and R. The response and control force are only relative to the ratio of α_1 to β_1. The optimal control forces may be obtained by minimizing the objective

function J in Eq. (28) with the constraints of Eq. (4). According to the principle of the extreme value, it can be obtained as follows:

$$U(t) = -R^{-1}B^T\lambda \tag{30}$$

$$\lambda = PZ(t) \tag{31}$$

$$U(t) = -GZ(t) \tag{32}$$

Let:

$$G = R^{-1}B^T P \tag{33}$$

where G is the optimal state feedback gain matrix; λ is $2n \times 1$ is Lagrange operator vector; P is $2n \times 2n$ is Riccati matrix, determined by:

$$\dot{P} = PA + A^T P - PBR^{-1}B^T P + Q \tag{34}$$

For a non-time-varying system, P can be considered as a constant matrix. Thus Eq. (34) can be simplified as:

$$PA + A^T P - PBR^{-1}B^T P + Q = 0 \tag{35}$$

To avoid time delay, Eq. (35) can be solved offline by iteration methods.

4. Numerical simulation

A complex system with two five-storey adjacent frame structures is considered as shown in Fig. 1. The mass and stiffness coefficients for each storey are m_i = 1.8×10^5 kg and $k_i = 9\times10^6$ kN/m, respectively. The damping ratio of structures is $\xi = 0.05$. The mass, equivalent stiffness and damping of rubber isolation floor of structure B are respectively 1.5×10^4 kg, 1.0×10^6 kN/m and 2×10^4 kN/m. The control actuator is located in the third floor. The scaled El Centro earthquake (north-south component) with maximum acceleration of $0.2g$ is used as the input excitation. The earthquake episode is 20 s. The coefficients of weight matrices are $\alpha_1 = 100$, $\beta_1 = 4 \times 10^{-5}$ respectively.

4. 1. Influence of time delay on LQR

To investigate the influence of time delay on LQR control, a time delay of 0.12 s is assumed during the control, which is 6 times of sampling steps. The responses histories of two cases (with time delay and without time delay) are compared and shown in Figs. 7-12.

From above simulation, it can be observed that the time delay has an obvious influence on the control of adjacent buildings. The displacement for top floor of structure A (fixed base) with time delay is 40 % larger than that without time delay, and the displacement for top floor of structure B (isolation bearing) with time delay is 20 % larger than that without the time delay. At the same time, the acceleration of top floor of structure A with time delay is also 20 % larger than that without time delay. Moreover, the time that the peak responses occurred between the two cases is quite different. For example, the peak displacement of structure A without time delay happens at 2.62 s, while that with time delay happens at 4.24 s (Table 1). This difference may results in a decrease of control effect or even a failure of control.

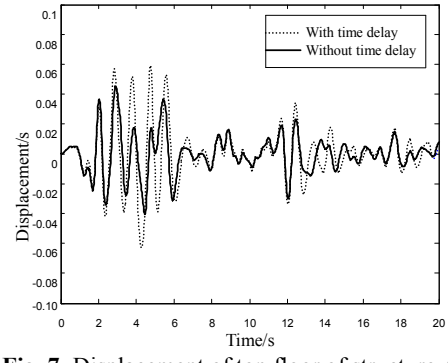

Fig. 7. Displacement of top floor of structure A

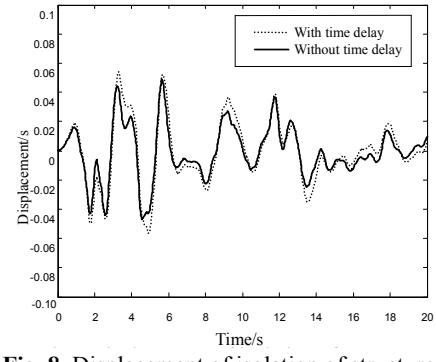

Fig. 8. Displacement of isolation of structure B

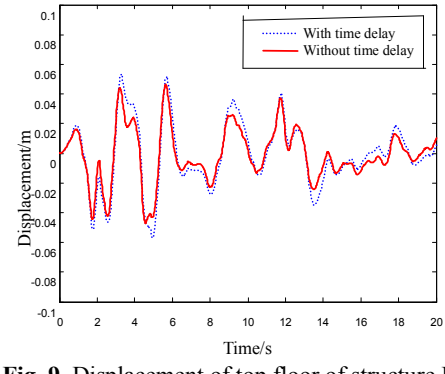

Fig. 9. Displacement of top floor of structure B

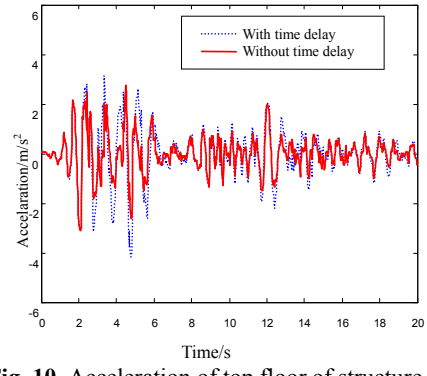

Fig. 10. Acceleration of top floor of structure A

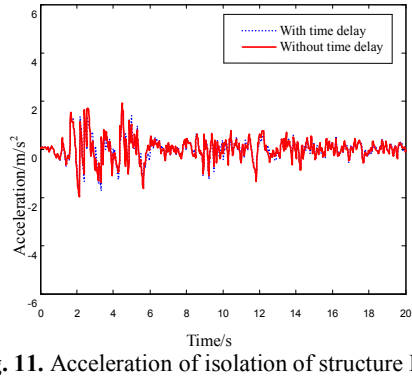

Fig. 11. Acceleration of isolation of structure B

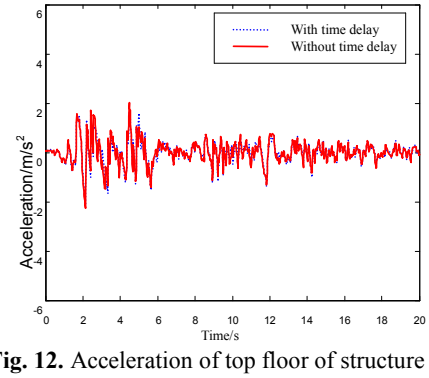

Fig. 12. Acceleration of top floor of structure B

Table 1. Peak value of response

	Peak displacement of top floor /cm		Peak acceleration of top floor /m/s^2	
	With time delay	Without time delay	With time delay	Without time delay
Structure A (Corresponding time)	6.32 (4.24 s)	4.51 (2.62 s)	4.16 (4.44 s)	3.10 (2.08 s)
Structure B (Corresponding time)	5.70 (5.12 s)	4.74 (5.98 s)	2.07 (1.98 s)	2.27 (4.24 s)

Therefore, the influence of time delay on vibration control, which the classical LQR method can not deal with, can not be neglected.

4. 2. Forecasting control based on grey model

It is assumed that the time delay is 0.12 s. The scaled El Centro earthquake (north-south component) with maximum acceleration of 0.2*g* is used as the input excitation. The responses history of structures with forecasting and without forecasting are calculated and compared in Figs. 13-18.

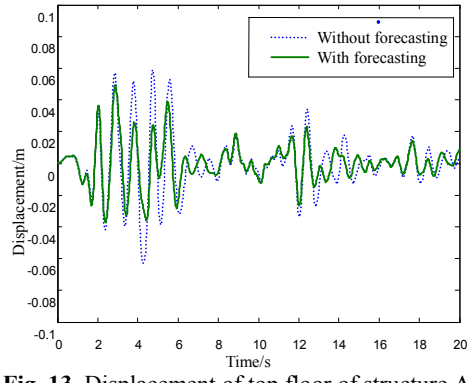

Fig. 13. Displacement of top floor of structure A

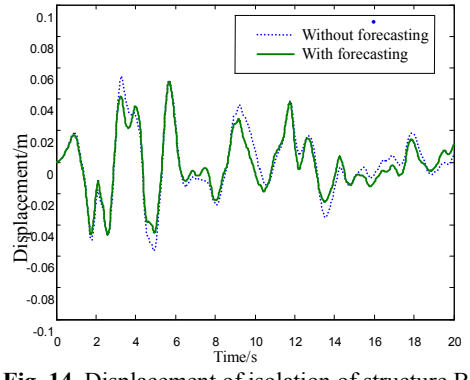

Fig. 14. Displacement of isolation of structure B

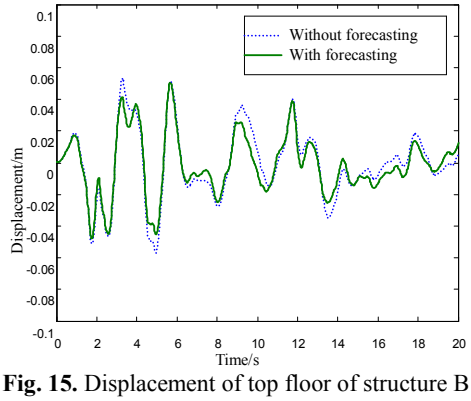

Fig. 15. Displacement of top floor of structure B

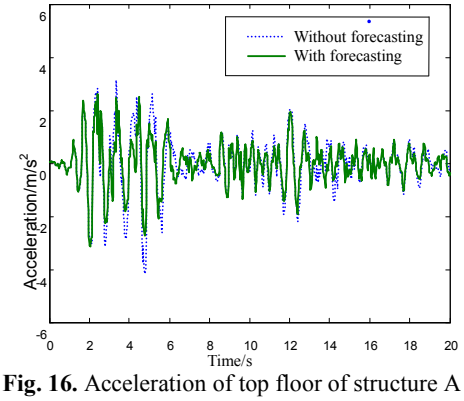

Fig. 16. Acceleration of top floor of structure A

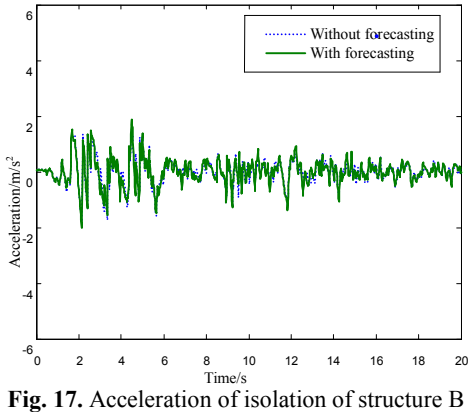

Fig. 17. Acceleration of isolation of structure B

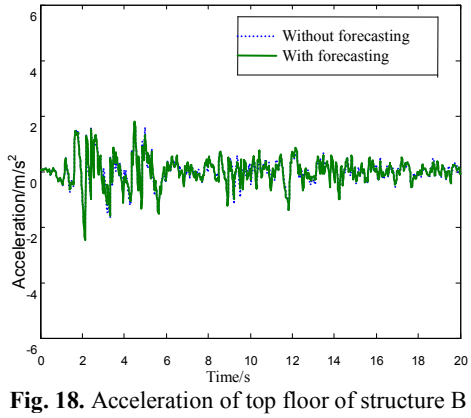

Fig. 18. Acceleration of top floor of structure B

Table 2. Response of forecasting control

	Peak displacement of top floor /cm		Peak acceleration of top floor /m/s^2	
	Without forecasting	With forecasting	Without forecasting	With forecasting
Structure A (Corresponding time)	6.32 (4.24 s)	4.92 (2.66 s)	4.16 (4.44 s)	3.16 (2.05 s)
Structure B (Corresponding time)	5.70 (5.12 s)	5.06 (5.75 s)	2.07 (1.98 s)	2.45 (2.07 s)

The simulation results indicate that the displacements of structures A and B with forecasting are much smaller than those without forecasting. It indicates that the forecasting control based on grey model can increase the effect of control effectively. To investigate the precision of grey forecasting, the comparison between the forecasting control with time delay and the LQR control without time delay is conducted as illustrated in Figs. 19-24.

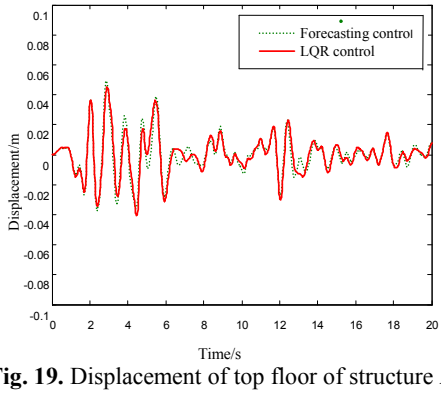

Fig. 19. Displacement of top floor of structure A

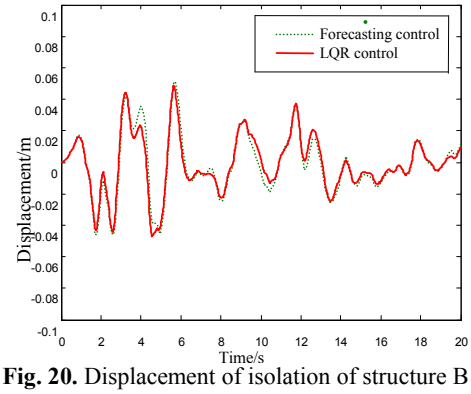

Fig. 20. Displacement of isolation of structure B

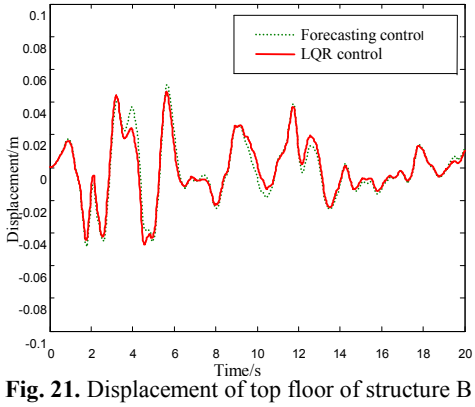

Fig. 21. Displacement of top floor of structure B

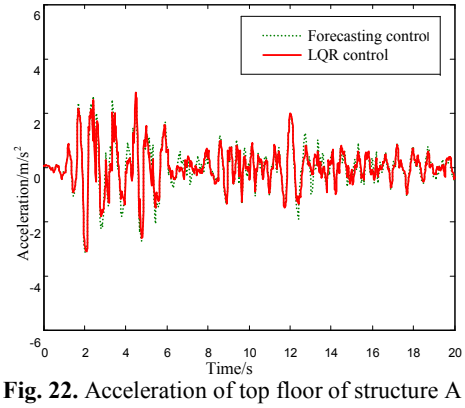

Fig. 22. Acceleration of top floor of structure A

Table 3. Comparison between LQR and forecasting control

	Peak displacement of top floor /cm			Peak acceleration of top floor /m/s^2		
	LQR No time delay	LQR Time delay	Forecasting control	LQR No time delay	LQR Time delay	Forecasting control
Structure A	4.51	6.32	4.92	3.10	4.16	3.16
(Corresponding time)	(2.62 s)	(4.24 s)	(2.66 s)	(2.08 s)	(4.44 s)	(2.05 s)
Structure B	4.74	5.70	5.05	2.27	2.07	2.45
(Corresponding time)	(5.98 s)	(5.12 s)	(5.75 s)	(4.24 s)	(1.98 s)	(2.07 s)

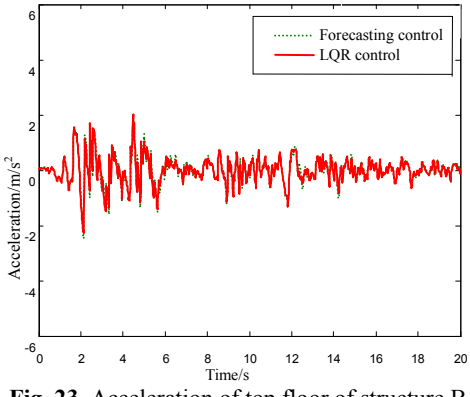

Fig. 23. Acceleration of top floor of structure B

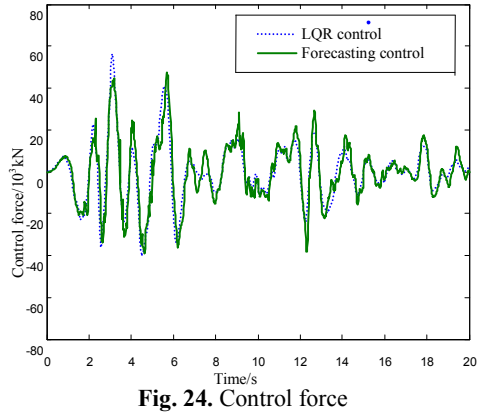

Fig. 24. Control force

From Figs. 19-24 it can be observed that the response of forecasting control with time delay is very close to that of LQR control without time delay. It indicates that the forecasting control based on grey model can reduce the influences of time delay on adjacent building vibration control.

4. 3. Comparison of the control precision

Defining that the response factor as ratio of the response of forecasting control with time delay to the response of LQR control without time delay, the response factors vary with time delay are presented in Fig. 25. Generally, the response factors increase with the accretion of time delay. When the forecasting is used, the trend of variety of response factor is much more gentle and stable than that of no forecasting.

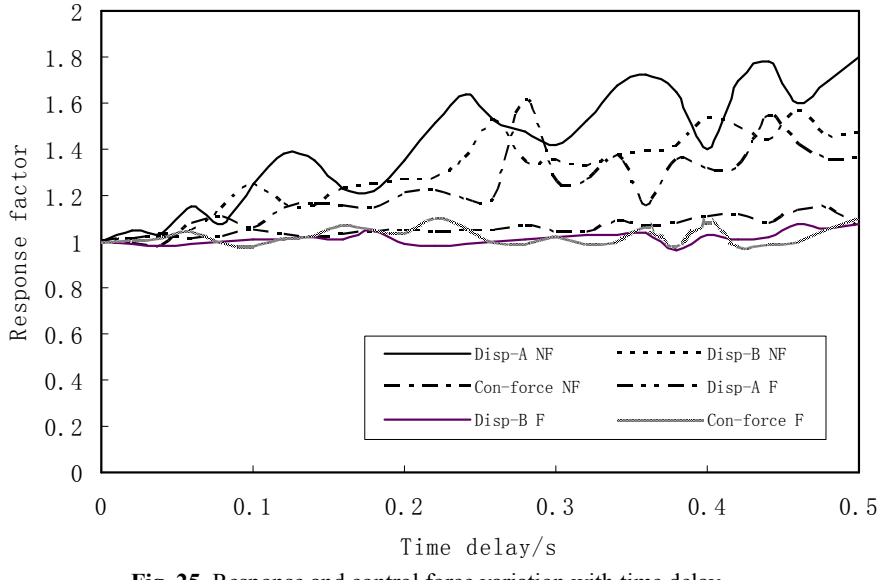

Fig. 25. Response and control force variation with time delay

Neural network is another widely used forecasting method in vibration control of civil engineering. To investigate the precision of optimal grey forecasting, the error of the response

histories (with time delay of 0.12 s) for method of neural network (with 500 steps of training) are computed and compared with the results of optimal grey model (Figs. 26 and 27). It can be observed that the forecasting precision of neural network is slightly better than that of grey model. But, generally, the errors for both methods are small enough to satisfy the requirement of civil engineering. Furthermore, the method of neural network needs a large quantity of data and multi-step training to achieve adequate forecasting precision. On the contrary, grey model are not dependent on accurate structural models and need only several samples. Hence, the forecasting based on optimal grey model has the advantage of precision and reliability, and it is suitable to be applied to the control forecasting of adjacent buildings.

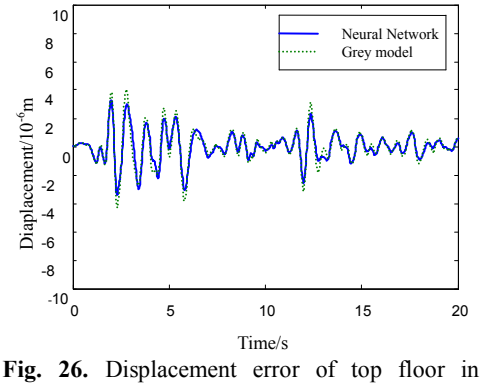

Fig. 26. Displacement error of top floor in structure A

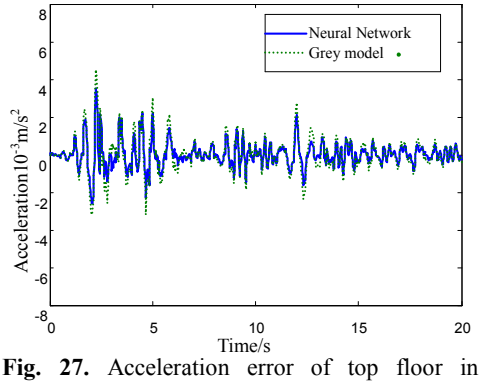

Fig. 27. Acceleration error of top floor in structure A

5. Conclusions

The vibration control of adjacent building has a larger time delay compared with control of single building. Time delay has an obvious influence on the control of buildings. It can reduce the efficiency of control or even result in a control failure.

Forecasting control based on optimal grey model can reduce the influence of time delay, and improve the efficiency of control. Additionally, the forecasting of optimal grey model can carry out a multi-step forecasting with a good forecasting precision, and it is applicable to vibration control with large or small time delay. Therefore, it is very suitable to the control of adjacent buildings.

Acknowledgement

This work was financially supported by the National Science Foundation of China under Grant No. 51108091.

References

[1] **Bertero V. V.** Observation of structural pounding. Proc. Int. Conf.: The Mexico Earthquake - 1985, ASCE, New York, 1986, p. 264-278.

[2] **Kasai K., Maison B. F.** Building pounding damage during the 1989 Loma Prieta earthquake. Engineering Structures, Vol. 19, Issue 1, 1997, p. 195-207.

[3] **Anagnostopoulos S. A.** Pounding of buildings in series during earthquakes. Earthquake Engineering and Structural Dynamics, Vol. 16, Issue 2, 1988, p. 443-456.

[4] **Wester B. D.** The dynamics of interstructural connection to prevent pounding. Earthquake Engineering and Structural Dynamics, Vol. 18, Issue 1, 1989, p. 687-699.

[5] **Xu Y. L., He Q., Ko J. M.** Dynamic response of damper-connected adjacent buildings under earthquake excitation. Engineering Structures, Vol. 21, Issue 4, 1999, p. 135-148.
[6] **Basili M., Angelis M. D.** Optimal passive control of adjacent structures interconnected with nonlinear hysteretic devices. Journal of Sound and Vibration, Vol. 301, Issue 11, 2007, p. 106-125.
[7] **Kobori T., Yamada T., Takenaka Y.** Effect of dynamic tuned connector on reduction of seismic response – application to adjacent office buildings. Proceedings of the Ninth World Conference Earthquake Engineering, Vol. 5, Tokio - Kioto, Japan, 1988, p. 773-778.
[8] **Zhang W. S., Xu Y. K.** Vibration analysis of two buildings linked by Maxwell model-defined fluid dampers. Journal of Sound and Vibration, Vol. 233, Issue 5, 2000, p. 775-796.
[9] **Ni Y. Q., Ko J. M., Ying Z. G.** Non-linear stochastic optimal control for coupled-structures system of multi-degree-of-freedom. Journal of Sound and Vibration, Vol. 274, Issue 2, 2004, p. 843-861.
[10] **Zou L. H., Bi G. H.** Optimal control for vibration of a base-isolated structure based on the grey forecasting. Journal of Vibration and Shock, Vol. 25, Issue 4, 2006, p. 179-185.
[11] **Deng J. L.** A novel GM(1,1) model for non-equigap series. Journal of Grey System, Vol. 9, Issue 1, 1997, p. 95-110.
[12] **Hao L. Y.** Sliding model control via grey prediction. Journal of Grey System, Vol. 8, Issue 1, 1996, p. 359-380.
[13] **Chen J. Y.** Tuning of prediction step in grey prediction controller using stochastic learning. Journal of Grey System, Vol. 4, Issue 1, 1996, p. 337-357.
[14] **Huang Y. P.** The application of multiple grey models to the control problems. Journal of Grey System, Vol. 7, Issue 4, 1995, p. 299-313.
[15] **Yi S. D.** Grey predictor controller for DC speed-control system. Journal of Grey System, Vol. 2, Issue 2, 1990, p. 189-215.